

다중 시퀀스 시그널링에 기초한 비동기 트래리스 부호화 DS/CDMA 시스템

정희원 최 상 호*, Costas N. Georghiades**

Multi-Sequence Signaling Based Asynchronous Trellis-Coded DS/CDMA System

Sangho Choe* *Regular Member*, Costas N. Georghiades**

요 약

Woerner는 비동기 트래리스 부호화 DS/CDMA (asynchronous trellis-coded DS/CDMA systems, A-TC-CDMA) 시스템에 낮은 상관도의 다중 시퀀스 시그널링인 배직교 시퀀스 (biorthogonal sequence)를 이용함으로써 단일 시퀀스 시그널링인 M-ary PSK에 비해 보다 개선된 시스템 성능을 얻을 수 있음을 보여주었다. 본 논문에서는 최근에 제안된 다중 시퀀스 시그널링 방식인 OPSM (orthogonal plane sequence modulation)과 배직교 시퀀스를 이용한 비동기 트래리스 부호화 CDMA 시스템 성능을 상호 비교 분석한다. 가입자 수신신호의 상호간섭 랜덤변수의 모멘트를 유도하고 그 결과 배직교 시퀀스 시그널링 방식에 비해 적은 수의 심볼당 시퀀스를 갖는 OPSM (orthogonal plane sequence modulation)이 시퀀스간 낮은 상호상관도 특성을 가짐을 보여준다. 또한 컴퓨터 시뮬레이션을 통하여 다중 시퀀스 시그널링 비동기 트래리스 시스템의 전력 효율 및 스펙트럼 효율을 비교 검증한다.

Key Words : Trellis-coded modulation (TCM), CDMA system, signaling sequence, power and/or spectral efficiency, cross-correlation.

ABSTRACT

Woerner had suggested an asynchronous trellis-coded DS/CDMA system based on a multi-sequence signaling, biorthogonal sequence, which is superior to single sequence signaling, such as M-ary PSK, due to their better cross-correlation properties. This paper analyzes and compares system performance between OPSM, a recently-presented multi-sequence signaling scheme, and biorthogonal sequence signaling. Interuser interference moments of the two schemes are derived and compared which verifies that OPSM, having smaller signature sequences per symbol than biorthogonal signaling, reduces cross-correlation. Numerical results compare the power and spectral efficiency of asynchronous trellis-coded DS/CDMA systems based on multi-sequence signaling.

I. Introduction

Trellis coded modulation (TCM), introduced by Ungerboeck in 1982 as a combined-technique of

modulation and coding, has applied to many telecommunication systems. TCM (or simply called as trellis-code (TC)) is recently widely used for high-rate wireless CDMA applications^{[2],[11]}, owing to its spectral efficiency

* School of Information, Communications & Electronics Engineering, The Catholic University of Korea (schoe@catholic.ac.kr),

** Department of Electrical Engineering, Texas A&M University (georghiades@ee.tamu.edu)

논문번호 : 030483-1104, 접수일자 : 2003년 11월 4일

superiority.

While synchronous or quasi-synchronous CDMA systems are signature sequence-limited, asynchronous CDMA systems, like W-CDMA, are interference-limited. Assuming reasonably the large processing gain N , because of user capacity reduction due to the interuser interference, practical A-TC-CDMA systems have enough room of increasing the signal space per signal symbol (depending on the number of signature sequences per symbol) without sacrificing the bandwidth efficiency^[2]. Hence, multi-sequence based TC schemes, such as orthogonal TC signaling^{[3],[4]} or biorthogonal TC signaling^[2], are more favorable than single-sequence based TC schemes like M -PSK TC^[1]. Woerner^[2] and Kim^[9] have shown that the A-TC-CDMA system based on biorthogonal signaling, due to its improved cross-correlation properties by the multi-sequence redundancy, results in better performance over other A-TC-CDMA systems as well as standard asynchronous convolutionally-coded CDMA systems (A-CC-CDMA). Recently, we introduced a new multi-sequence TC called orthogonal plane sequence modulation (OPSM)^[5] for which in this paper we applied to asynchronous TC-CDMA system and compared it to biorthogonal sequence based asynchronous TC-CDMA systems.

We derive Chernoff bounds on the bit-error-rate performance of the proposed A-TC-CDMA system by using Gaussian quadrature rules. OPSM signalings^[5] are called as LPMPSK, where L is the number of sequences per symbol and M is the number of signal points per sequence. We mainly compare between OPSM TC with a constraint of $M=4$, i.e. having four signal points per sequence (4-PSK per sequence), and biorthogonal TC; then the signal space of OPSM is just one half of biorthogonal signaling while keeping the same distance profiles. Hence, compared to existing multi-sequence based A-TC-CDMA, OPSM based A-TC-CDMA improves cross-correlation properties. In particular, as data rate R_b increases the BER performance

of the proposed A-TC-CDMA improves further. The proposed A-TC-CDMA also improves system adaptability by providing several options per data rate: e.g. 2P8PSK/4P4PSK/8P2PSK (=16 biorthogonal) for 3 bits/s/Hz. Numerical results also show that the performance of the proposed system is superior to biorthogonal based A-TC-CDMA systems as well as standard A-CC-CDMA systems.

In Sect. II, III we illustrate system model and performance analysis of the OPSM based A-TC-CDMA system, respectively. We present numerical results of our system and compare with conventional multi-sequence signaling based A-TC-CDMA systems and A-CC-CDMA systems in Sect. IV. Finally, we conclude with Sect. V.

II. System Model

The proposed A-TC-CDMA is based on L orthogonal signature sequences, called as LPMPSK (L planar M -ary PSK), so the signal space of that signal would be the real $2L$ -dimensional Euclidean space R^{2L} ^[5]. As L signature sequences, we could use either perfect orthogonal sequences like Walsh functions or pseudo-orthogonal sequences like Gold-sequences since there is no big performance difference between two sequences^[2].

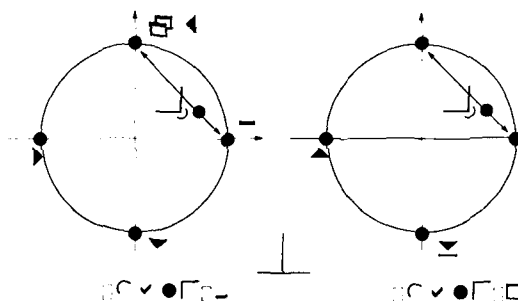


Fig. 1 Signal constellation for 2P4PSK.

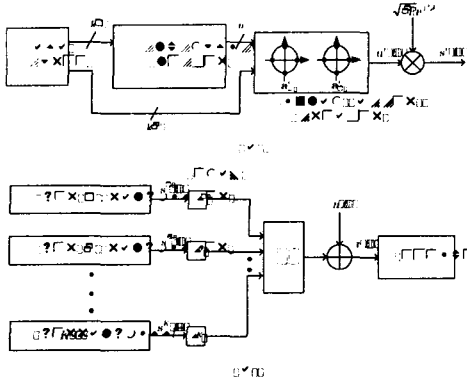


Fig. 2 (a) User *i* transmitter block diagram.
(b) General system architecture.

Assuming the *k*th user transmits a symbol $u_{l,m}$ where $l=0, \dots, L-1$ and $m=0, \dots, M-1$, its signal representation becomes $u_{l,m}^k(t) = e^{j\phi_m^k} \sum_{n=0}^{N-1} a_{l,n}^k p_{T_c}(t - nT_c)$, where $a_{l,n}^k$ represents the *n*th chip of the *k*th user *l*th signature sequence vector (sequence component): $a^k = \{a_{l,0}^k, a_{l,1}^k, \dots, a_{l,N-1}^k\}$ and $\phi_m^k = m\pi/M$, ($m=0, \dots, M-1$) represents the phase component of the *k*th user signal; *N* is the length of sequence, T_c is the chip period, and $p_{T_c}(\cdot)$ is the chip waveform function. For instance, Fig. 1 shows the 2P4PSK signal constellation that consists of two signal planes, each containing a 4-PSK constellation. The transmitter of OPSM TC has the same structure (see in Fig. 2 (a)) as conventional TC schemes^[7], except that the signal mapper maps an input vector (convolutional encoder output vector plus parallel transition vector) into a combination of phase modulation component ϕ_m and sequence modulation component a_l (whose time-axis notation is $a_l(t)$). Note that differing from conventional TC-CDMA, the spreading function is built into the signal mapper, as depicted in Fig. 2(a).

Fig. 2(b) displays the general TC-CDMA system structure. Assuming the transmit symbol of

User *i* (desired user) is transmitted the corresponding received signal (omitting signal indices *l* and *m* for simplicity) then becomes

$$r(t) = \sum_{k=1}^K \sqrt{2P} \text{Re} [u^k(t) e^{j(w_c(t-\tau^k) + \theta^k)}] + n(t)$$

where *K* is the number of users, *P* is the signal power, and w_c is the carrier frequency; τ^k and θ^k are the time delay and the phase delay of the *k*th user, respectively, and when assuming asynchronous systems the time delay (τ^k) of user signal is uniformly distributed over a symbol period $T_s = NT_c$; $n(t)$ is the AWGN channel noise with a two-sided spectral density $N_0/2$.

We consider a coherent matched-filter receiver that consists of a bank of $2L$ correlators, see in detail in^[5], since the established signaling scheme is based on *L* signature sequences. That receiver output becomes a soft decision output vector with an order of $2L$; then the channel output vector is decoded by a Viterbi decoder. Coherent detection is assumed for User *i* whose time delay τ^i is zero.

II. Performance Analysis

1. Pairwise Error Probability

Let us assume that a signal on the *l*th plane of User *i* will be transmitted and recovered at the receiver. The correlation output vector of User *i* at the *p*th instance can be specified as $Y_{\rho}^i = \{Y_{j,\rho}^i; j=0, \dots, L-1\}$, where each element of that output vector can be represented by

$$Y_{j,\rho}^i = \begin{cases} \sqrt{E_s} e^{j\phi_s^i} + \frac{\sqrt{E_s}}{T_s} \sum_{k=1}^K \{ R_{j,l_{\rho-1}}^{i,k}(\tau^k) e^{j\beta_s^k} + \tilde{R}_{j,l_{\rho}}^{i,k}(\tau^k) e^{j\beta_s^k} \} + \eta_{j,\rho}^i, & \text{for } j=l \\ -\frac{T_c \sqrt{E_s}}{T_s} e^{j\phi_s^i} + \frac{\sqrt{E_s}}{T_s} \sum_{k=1}^K \{ R_{j,l_{\rho-1}}^{i,k}(\tau^k) e^{j\beta_s^k} + \tilde{R}_{j,l_{\rho}}^{i,k}(\tau^k) e^{j\beta_s^k} \} + \eta_{j,\rho}^i, & \text{for } j \neq l \end{cases} \quad (1)$$

in which E_s is the symbol energy and $\eta_{j,\rho}^i$ is the

noise component of the j th plane with a variance of $N_0/2$; the signal phase of the k th user is $\beta_p^k = \phi_p^k + \theta^k - w_c \tau^k = \phi_p^k + \theta^k$, where the k th user signal phase term is $\phi^k = \{0, \pi/2, \pi, 3\pi/2\}$ and the phase delay θ^k , dropping the prime (') without loss of generality, is a uniformly distributed random variable in the range of $[0, 2\pi)$; l_{p-1} and l_p represent the k th user signal plane index at the $(p-1)$ th and the p th time instance, respectively. For the sake of mathematical simplicity, we assume that these two consecutive plane indices of the k th user are the same: $l = l_{p-1} = l_p$. $R(\cdot)$ and $\tilde{R}_{j,l}^{i,k}(\cdot)$ represent the even and odd continuous-time partial cross-correlation functions^[1], respectively, between the i th user j th plane signal and the k th user l th plane signal. Differing from quasi-synchronous CDMA systems^[5], we cannot drop the plane indices from Eq. (1) since in A-TC-CDMA systems there is no guarantee of pseudo-orthogonality (orthogonality) between two different user signals due to the time delay.

This correlation output vector can be also represented as a vector^[5] like

$$\mathbf{Y}_p^i = \mathbf{G}_p^i + \mathbf{V}_p^i + \boldsymbol{\eta}_p^i \quad (2)$$

where \mathbf{G}_p^i is the desired signal (User i) symbol vector, \mathbf{V}_p^i is the interuser interference vector, and $\boldsymbol{\eta}_p^i$ is the noise vector whose element on each plane has a variance of $N_0/2$; the size of all those vectors is L . Let us assume that we use a rectangular chip waveform signal.

We apply Gaussian quadrature rules (GQR)^[7] to obtain a performance bound, since for practical systems we cannot assume Gaussian statistics for the interuser interference. As a result, the pairwise error probability, whose detail derivations are given in Appendix A, between a (normalized) correct symbol sequence $\mathbf{g} = \{\mathbf{g}_p; p=1, \dots, N_p\}$,

where N_p is the size of symbol sequence, and a (normalized) incorrect symbol sequence $\tilde{\mathbf{g}} = \{\tilde{\mathbf{g}}_p; p=1, \dots, N_p\}$ results in

$$P(\mathbf{g} \rightarrow \tilde{\mathbf{g}}) \leq \prod_{p \in C} \exp\left[-\lambda(1-\lambda) \frac{E_s}{N_0} \|\mathbf{g}_p - \tilde{\mathbf{g}}_p\|^2\right] \cdot \sum_{j=1}^N W_{i,p} \exp\left(-2\lambda \frac{E_s}{N_0} \zeta_{j,p}\right) \quad (3)$$

where $\mathbf{g}_p = \mathbf{G}_p/\sqrt{E_s}$, $\tilde{\mathbf{g}}_p = \tilde{\mathbf{G}}_p/\sqrt{E_s}$ and C is the set of p such that $\mathbf{g} \neq \tilde{\mathbf{g}}$; $W_{j,p}$ and $\zeta_{j,p}$ are obtained from Eq. (6) of Appendix A. We use a numerical optimization approach^[1] to get λ (= Chernoff parameter) tightening the bound.

To compute BER results, we use the generalized transfer function $T(Z, D)$ based on the product trellis of the trellis-coded system^[5] and then use

$$P_b \leq \frac{1}{n} \frac{\partial \overline{T}(Z, D)}{\partial Z} \Big|_{Z=1}$$

where n is the number of bits per symbol and the overbar indicates that the transfer function bound has been averaged over the interuser interference.

2. Interuser Interference Moments

To compare the cross-correlation characteristics of the proposed signaling LPMPK and conventional biorthogonal signaling, we derive the interuser interference moments of the normalized interuser interference random variable $\mathbf{v} = \mathbf{V}/\sqrt{E_s}$ whose detail derivations are illustrated at Appendix B.

Table 1. Comparison of Interuser Interference Moments between Biorthogonal Signaling and OPSM Signaling

m	R _b =2bits/sec/Hz		R _b =3bits/sec/Hz	
	8-ary Bio.	2P4PSK	16-ary Bio.	4P4PSK
0	1.00e+00	1.00e+00	1.00e+00	1.00e+00
2	2.10e-02	2.08e-02	2.10e-02	2.08e-02
4	1.58e-03	1.57e-03	1.59e-03	1.50e-03
6	2.18e-04	2.11e-04	2.21e-04	1.96e-04
8	4.51e-05	4.16e-05	4.56e-05	3.79e-05
10	1.25e-05	1.10e-05	1.26e-05	9.75e-06
12	4.38e-06	3.62e-06	4.41e-06	3.15e-06
14	1.85e-07	1.44e-06	1.86e-06	1.22e-06
16	9.13e-07	6.70e-07	9.15e-07	5.55e-07
18	5.14e-07	3.55e-07	5.14e-07	2.86e-07
20	3.23e-07	2.10e-07	3.24e-07	1.65e-07

For a fair comparison, the same alphabet size and same complexity is assumed in both schemes; to keep the same distance profiles in two schemes *M* is assumed 4. Let us assume the sequence length *N* is 63 and the number of users *K* is 5. The interuser interference moments of two 2 bits/sec/Hz schemes (8-ary biorthogonal and 2P4PSK) and two 3 bits/sec/Hz schemes (16-ary biorthogonal and 4P4PSK) are compared each other in Table-[\ref{tab:mom}](#); all odd moments are zero, since the interference random variable assumes to be evenly-distributed. One can observe that the value of all moments in the proposed signaling at *m*>0 (where *m* is the order of moments) is less than biorthogonal signaling. We can observe that the difference of the interuser interference moments between the two signaling schemes gets greater as data rate (*R_b*) increases, which implies that the BER (bit-error-rate) performance of the proposed signaling becomes better at high rates (> 3 bits/sec/Hz).

2.1 Pairwise Error Probability Derivation

Let us derive the Chernoff bounds on the pairwise error probability between a correct symbol sequence *g* and an incorrect symbol sequence \tilde{g} of the proposed A-TC-CDMA system

based on OPSM. Let us assume *M*=4 for simplicity but it is easily extensible. Based on the channel output signal vector Eq. (2), we can define the pairwise error probability, dropping user index *i* for simplicity, as follows[5]:

$$P(\mathbf{g} \rightarrow \tilde{\mathbf{g}}) \leq \frac{1}{2} \prod_{p \in C} \exp[-\lambda E_s (1 - \lambda N_0) \|\mathbf{g}_p - \tilde{\mathbf{g}}_p\|^2] \cdot E\left\{ \exp\left[-2\lambda E_s \sum_{j=0}^{L-1} \text{Re}\{v_{j,p}(\tilde{g}_{j,p} - \tilde{g}_{j,p})^*\}\right] \right\} \tag{4}$$

where $\mathbf{g}_p = \mathbf{G}_p / \sqrt{E_s}$, $\tilde{\mathbf{g}}_p = \tilde{\mathbf{G}}_p / \sqrt{E_s}$ the normalized interuser interference vector $\mathbf{v}_p = \mathbf{V}_p / \sqrt{E_s}$ and *C* is the set of path *p* such that $\mathbf{g} \neq \tilde{\mathbf{g}}$.

Let us reorganize the expectation on the right hand side of Eq. (4) as follows:

$$E \left\{ \exp\left[-2\lambda E_s \sum_{j=0}^{L-1} \text{Re}\{v_{j,p} \delta_{j,p}^*\}\right] \right\} = E\left\{ \exp\left[-\alpha \text{Re}\left\{ \sum_{k=1}^K \sum_{j=0}^{L-1} \delta_{j,p}^* R_{j,i}^{i,k}(\tau^k) e^{j\phi_i} + \tilde{R}_{j,i}^{i,k}(\tau^k) e^{j\phi_i} \right\}\right] \right\} = E\left\{ \exp(-\alpha \mathbf{y}_p) \right\} \tag{5}$$

where

$$\mathbf{y}_p = \text{Re} \left\{ \sum_{k=1}^K \sum_{j=0}^{L-1} \delta_{j,p}^* \left\{ R_{j,i}^{i,k}(\tau^k) e^{j\phi_i} + \tilde{R}_{j,i}^{i,k}(\tau^k) e^{j\phi_i} \right\} \right\},$$

$\alpha = 2\lambda E_s / N$, and $\delta_{j,p} = \mathbf{g}_{j,p} - \tilde{\mathbf{g}}_{j,p}$ notice that the time delay τ^k is the normalized version by a chip period *T_c*. Since we do not know the statistics of random variable \mathbf{y}_p so to evaluate Eq. (5) we use Gaussian quadrature rules (GQR)^[7] based on the moments of that random variable. Following the similar procedure as Appendix C in^[5], we can easily get the moments of the random variable \mathbf{y}_p as follows:

$$E[\mathbf{y}_p^{2m}] \simeq \frac{1}{4^m} \binom{2m}{m} \sum_{\mathbf{a} \in \mathbf{A}} \left(\frac{m!}{a_1! \cdots a_K!} \right)^2 \quad (6)$$

$$\cdot \prod_{k=1, k \neq i}^K \left\{ \sum_{l=0}^{a_k} \binom{a_k}{l}^2 f^k(d_{sq}) \right\}$$

where $f^k(d_{sq})$ becomes

$$f^k(d_{sq}) = \begin{cases} (d_{sq})^{\alpha} P_s E\{ (R_{\alpha}^{i,k}(\tau^k))^{2l} (R_{\beta}^{j,k}(\tau^k))^{2(a_k-l)} \} \\ + P_d E\{ ((R_{\alpha}^{i,k}(\tau^k))^2 + (R_{\beta}^{j,k}(\tau^k))^2)^l \\ \cdot ((R_{\alpha}^{i,k}(\tau^k))^2 + (R_{\beta}^{j,k}(\tau^k))^2)^{a_k-l} \} \\ \text{for } d_{sq} = 2 \\ (d_{sq})^{\alpha} E\{ (R_{\alpha}^{i,k}(\tau^k))^{2l} (R_{\alpha}^{i,k}(\tau^k))^{2(a_k-l)} \} \\ \text{for } d_{sq} = 4 \end{cases} \quad (7)$$

in which $\alpha = \{0, \dots, L-1\}$ and $\beta = \{0, \dots, L-1\}$ but $\alpha \neq \beta$, P_s is the probability that in the OPSM signal the two signal points with a distance $d_{sq} = 2$ place on the same signal plane and P_d is the probability that two signal points with a distance $d_{sq} = 2$ place on two different signal planes; so for OPSM, $P_s = 1/(2(L-1) + 1)$ and $P_d = 2(L-1)/(2(L-1) + 1)$. Also note that we need to average the expectations of Eq. (7) for all possible signature sequences.

The N_m moments of \mathbf{y}_p obtained from Eq. (6), where $N_m = 2N_c + 1$, yield N_c pairs of weight W_j and node ζ_p from which Eq. (5) becomes^[11]: Eq.

$$(5) = \sum_{j=1}^N W_{j,p} \exp(-2\lambda E_s \zeta_{j,p}).$$

Finally, from Eq. (4), by letting $\lambda' = \lambda/N_0$ and dropping the primes, we can obtain the pairwise error probability Eq. (3) in Sect. III.

2.2 Comparison of Interuser Interference

For a fair comparison, we consider the interuser interference moments of between the proposed signaling, OPSM with a constraint of $M=4$, and biorthogonal signaling. Let us first calculate the interuser interference moments of the proposed signaling. Regarding the normalized interuser interference random variable vector \mathbf{v}_p i.e.

$\mathbf{v}_p = \mathbf{V}_p / \sqrt{E_s}$, we will calculate its moments as a measure of interuser interference characteristics. In that signaling, the j th element of that normalized interference random variable vector $\mathbf{v}_p = (v_{0,p}, \dots, v_{L-1,p})$ at the p th instance becomes

$$v_{j,p} = \frac{1}{N} \operatorname{Re} \left\{ \sum_{k=1, k \neq i}^K (x_{p-1}^k R_{i,i}^{j,k}(\tau^k) + x_p^k R_{i,i}^{j,k}(\tau^k)) e^{j\theta^k} \right\}$$

$$= \frac{(z_p + z_p^*)}{2N} \quad (8)$$

in which $j = 0, \dots, L-1$, x_q is the phase component of the modulation symbol at the q th instance, where q is p or $p-1$: $x_q = e^{j\phi_q}$, $\phi_q = \{0, \pi/2, \pi, 3\pi/2\}$, and

$$z_p = \sum_{k=1, k \neq i}^K (x_{p-1}^k R_{i,i}^{j,k}(\tau^k) + x_p^k R_{i,i}^{j,k}(\tau^k)) e^{j\theta^k}.$$

For simplicity, we can drop the subscript p under the assumption of symbol-by-symbol independence.

$$E[\mathbf{v}^{2m}] = \frac{1}{(2N)^{2m}} \sum_{n=0}^{2m} \binom{2m}{n} E[(z)(z^*)^{m-n}]$$

$$\simeq \frac{1}{(2N)^{2m}} \binom{2m}{m} \sum_{\mathbf{a} \in \mathbf{A}} \left(\frac{m!}{a_1! \cdots a_K!} \right)^2$$

$$\cdot \prod_{k=1, k \neq i}^K \left\{ \sum_{d=0}^{a_k} \binom{a_k}{d}^2 E[(R_{i,i}^{j,k}(\tau^k))^{2d} (R_{i,i}^{j,k}(\tau^k))^{2(a_k-d)}] \right\}$$

[for OPSM] (9)

Assuming the random variable \mathbf{v} is evenly distributed, we only need even moments of \mathbf{v} that is given by in which \mathbf{A} is the set of sequence $\mathbf{a} = \{a_k; k=1, \dots, K, \text{ and } k \neq i\}$ such that $\sum_{k, k \neq i} a_k = m$.

Second, for biorthogonal schemes^[2] let us obtain the moments of the normalized interference random variable vector \mathbf{v}_p . Assuming M -ary biorthogonal signaling, its signal constellation consists of $L = M/2$ real Euclidean signal planes.

The transmit signal x_p in biorthogonal signaling is antipodal: $x_p \in \{\pm 1\}$. Let us assume a signal on the j th signal plane is transmitted. Then we can easily obtain the j th element of v_p as follows:

$$v_{i,b} = \frac{1}{N} \sum_{k=1, k \neq i}^K \{x_{b-1}^k R_{i,i}^{i,k}(\tau^k) + x_b^k \tilde{R}_{i,i}^{i,k}(\tau^k)\} \cos \theta^k \quad (10)$$

in which $j=0, \dots, L-1$ and x_q is the antipodal signal component at the q th instance, where q is p or $p-1$. By following the same procedures as OPSM, one can obtain the interuser interference moments of biorthogonal signaling as follows:

$$E[v^{2m}] = \frac{1}{N^{2m}} \sum_{\substack{a \in A \\ a_i \neq a, k \neq i}} \left(\frac{2m!}{2a_1! \dots 2a_K!} \right) \cdot \prod_{k=1, k \neq i}^K \left\{ \sum_{l=0}^{a_k} \frac{1}{2^{2a_l}} \binom{2a_k}{2l} \binom{2a_k}{a_k} \cdot E[(R_{i,i}^{i,k}(\tau^k))^{2l} (\tilde{R}_{i,i}^{i,k}(\tau^k))^{2(a_k-l)}] \right\} \quad (11)$$

[for Biorthogonal]

in which A is the set of sequence $a = \{a_k, k=1, \dots, K \text{ and } k \neq i\}$ such that $\sum_{k=1, k \neq i}^K a_k = m$.

III. Numerical Results

We compare the numerical results between the proposed A-TC-CDMA based on OPSM TC and conventional A-TC-CDMA based on biorthogonal TC^[6] as well as standard A-CC-CDMA based on BPSK.

For a fair comparison we employ the same Ungerboeck's systematic convolutional encoders with feedback. In particular, the 4-state rate 1/2 convolutional codes and the 8-state rate 2/3 convolutional codes are implemented. Also we

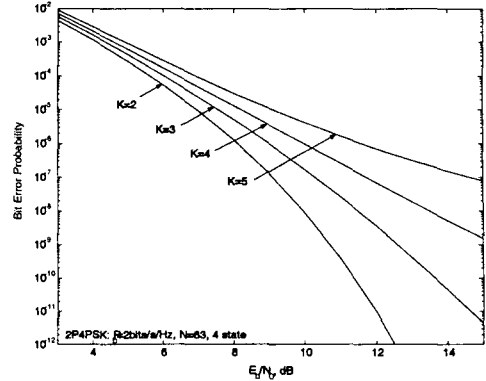


Fig. 3 Upper bounds on bit error probability of rate 2/3 2P4PSK TC with 4-state 1/2 convolutional code as a function of the number of users (K).

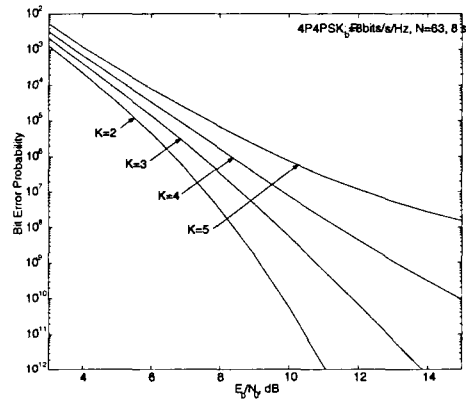


Fig. 4 Upper bounds on bit error probability of rate 3/4 4P4PSK TC with 8-state 2/3 convolutional code as a function of the number of users (K).

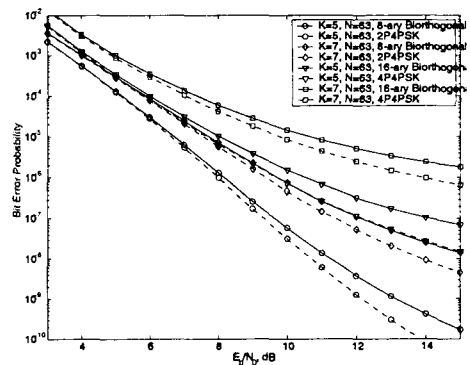


Fig. 5 Performance comparison at both rate 2/3 8-ary biorthogonal TC vs. rate 2/3 2P4PSK TC and rate 3/4 16-ary biorthogonal TC vs. rate 3/4 4P4PSK TC under the same 8-state 2/3 convolutional code as a function of the number of users (K).

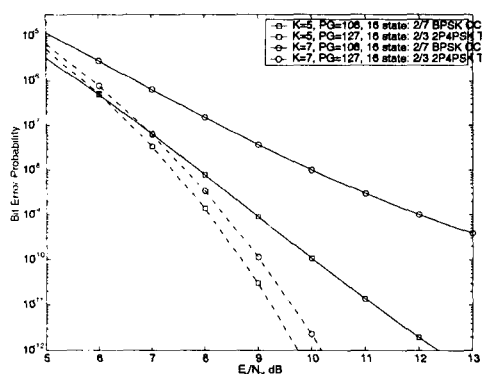


Fig. 6 Performance comparison between 16-state rate 2/7 BPSK CC system and 16-state rate 2/3 2P4PSK TC system as a function of the number of users (K).

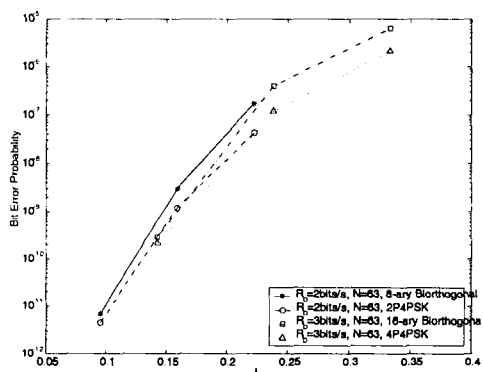


Fig. 7 BER performance as a function of normalized offered traffic $L (= R_b \cdot K / N)$ for biorthogonal TC and OPSM TC schemes both at rate 2/3 TC and at rate 3/4 TC, respectively, with the same 8-state 2/3 convolutional code.

assume the same data rate and same sequence length for both systems. As pseudo-random orthogonal sequences in our simulation, we use the [15] preferentially-phased Gold-sequences.

Fig. 3 and Fig. 4 show the BER performance of the 4-state rate 2/3 2P4PSK TC and the 8-state rate 3/4 4P4PSK TC as a function of the number of users K , respectively; the convolutional code implemented is a 4-state rate 1/2 code and a 8-state rate 2/3 code, respectively, and the sequence length of both schemes is the same $N=63$. We compare the BER performance of both the rate 2/3 2P4PSK TC and the rate 2/3 8-ary biorthogonal TC in Fig. 5 with respect to the number of users K , under the same 8-state

rate 2/3 convolutional code and same sequence length $N=63$; Fig. 5 also compares the rate 3/4 4P4PSK TC and the rate 3/4 16-ary biorthogonal TC, under the same 8-state rate 2/3 convolutional code and the same sequence length $N=63$. We can see that as R_b increases, the relative performance gain of our scheme over biorthogonal scheme becomes greater. For example, for $K=7$ and $N=63$, the performance gain is about 0.2~0.3 dB at 2 bits/sec/Hz and is 1.0 dB at 3 bits/sec/Hz, based on 10^{-5} BER.

We also compare the theoretical bounds of a 16-state rate 2/3 2P4PSK TC to a convolutionally-coded CDMA system, i.e. a 16-state rate 2/7 BPSK CC^[11], in Fig. 6, as a function of the number of users K ; the PG = 108.5 of rate 2/7 BPSK CC (Assuming the sequence length per symbol = 31, PG = 31*1/code rate) and the PG = 127.5 ($N = 255$ assumed) of 2/3 2P4PSK TC are similar. Fig. 6 shows that the proposed trellis-coded system is still superior to the low-rate convolutionally-coded system, except at low SNR at small number of users, e.g. for SNR > 6 dB at $K=5$.

For a fair spectral efficiency comparison between CDMA systems we compare BER performance in terms of the system loading for which the normalized offered traffic $L = R_b \cdot K / N$ ^[2], where K is the number of users. Fig. 7 shows BER performance versus L between conventional A-TC-CDMA systems and OPSM based A-TC-CDMA system, where we assume $E_b/N_0 = 10$ dB, $N=63$, and the same 8 state 2/3 convolutional codes. One can observe that OPSM TC outperforms conventional biorthogonal TC; especially, the increase of L makes the performance difference between two schemes further.

IV. Conclusion

In this paper, the multi-sequence signaling schemes for asynchronous trellis-coded CDMA

(A-TC-CDMA) system have been investigated. Since the signal space of OPSM (Orthogonal Plane Sequence Modulation)^[5] reduces less than a half of conventional biorthogonal signaling while keeping the same distance profiles, OPSM in asynchronous channels yields the smaller interuser interference moments compared to biorthogonal schemes. Hence, the OPSM based A-TC-CDMA provides better power and/or spectral efficiency than conventional A-TC-CDMA.

We derive the Chernoff bounds and execute Monte-Carlo simulation for BER performance of the OPSM based A-TC-CDMA, which proves that OPSM is superior to other multi-sequence signalings as well as M -ary PSK; as data rate R_b increases the performance gap becomes greater.

References

[1] G. D. Boudreau, D. D. Falconer, and S. A. Mahmoud,, "A comparison of trellis coded versus convolutionally coded spread-spectrum multiple-access systems", *IEEE J. on Select. Areas in Commun.*, 8(4), pp. 628-639, 1990.

[2] B. D. Woerner and W. E. Stark, "Trellis-coded direct-sequence spread-spectrum communications," *IEEE Trans. Commun.*, 42(12), pp. 3161-3170, Dec. 1994.

[3] P. K. Enge and D. V. Sarwate, "Spread spectrum multiple-access performance of orthogonal codes - linear receivers," *IEEE Trans. Commun.*, 35(12), pp. 1309-1318, Dec. 1987.

[4] S. L. Miller, "Design and analysis of trellis codes for orthogonal signal sets," *IEEE Trans. Commun.*, 43(2/3/4), pp. 821-827, Feb./Mar./Apr. 1995.

[5] S. Choe and C. N. Georghiades, "On the performance of a novel quasi-synchronous trellis-coded CDMA system," *IEEE Trans. Commun.*, 50(12), pp. 1984-1993, Dec. 2002.

[6] S. Choe, C. N. Georghiades, and K. Narayanan, "Improved upper bounds on the probability for the biorthogonal trellis-coded

CDMA system," *IEEE Commun. Lett.*, 6(9), pp. 361-363, Sept. 2002.

[7] G. Ungerboeck, "Channel coding with multilevel/phase signals," *IEEE Trans. Inform. Theory*, 28(1), pp. 55-67, Jan. 1982.

[8] M. Kavehrad, "Performance of nondiversity receivers for spread spectrum in indoor wireless communications," *AT&T Tech. J.*, 64(6), pp. 1181-1210, July-Aug. 1985.

[9] K. S. Kim, L. Song, H. G. Kim, Y. H. Kim, and S. Y. Kim, "A multiuser receiver for trellis-coded DS/CDMA systems in asynchronous channels," *IEEE Trans. Commun.*, 49(3), pp. 844-855, May 2000.

최 상 호(Sangho Choe)

정회원

1984년 2월 : 한양대학교 전자공학과 석사
 1984년 3월~1994년 2월 : 국방과학연구소
 1994년 3월~1996년 1월 : 한국전자통신연구소
 2001년 5월 : Texas A&M University, 공학박사
 2001년 7월~2002년 6월 : RadioCosm Inc., San Jose, CA
 2003년 3월~현재 : 가톨릭대학교 정보통신전자공학 부 조교수

<주관심분야> 이동통신, 통신신호처리, 무선통신시스템 SoC설계

Costas N. Georghiades

비회원

1985년 월~현재 : Texas A&M University, Electrical Eng. Dept., Professor

<주관심분야> Receiver Design, Distributed Source Coding, Adaptive Modulation and Coding.